# Effect of Carrier Concentration on the Raman Frequencies of Si and Ge†

Fernando Cerdeira* and Manuel Cardona*
*Department of Physics, Brown University, Providence, Rhode Island* 02912
(Received 11 June 1971)

The first-order Raman spectrum of Ge and Si has been investigated as a function of carrier concentration. In $p$-type materials we observed large broadenings of the Raman line and large shifts to higher frequencies of the Stokes line. We attribute these effects to the splitting of the valence band produced by the $\vec{k} \simeq 0$ optical phonon in a manner similar to the effects of doping on the $C_{44}$ elastic constant discussed by Keyes. From these results it is possible to estimate the coupling constant $d_0$ between optical phonons and holes. The $\vec{k} \simeq 0$ phonon should also produce a splitting of the conduction band of Ge (but not of Si). However, for a given impurity concentration, the shifts observed in $n$-type materials are much smaller than those for $p$-type materials. The absence of large effects is probably due to the low rate of intervalley scattering. An effect on $n$-type Si related to the splitting of the $X_1$ conduction-band degeneracy by the phonon is also discussed and compared with the analogous effect on the elastic constants. It is shown that the internal stress parameter $\zeta$ is also affected by doping.

## I. INTRODUCTION

Several years ago, Keyes[1] pointed out that the elastic properties of semiconductors depend on the free-electron or hole concentration. The strain produced by an acoustic wave or a uniaxial stress produces changes in the electronic energy bands of semiconductors, which can be represented by deformation-potential Hamiltonians.[2] In Si and Ge the shear strain shifts equivalent conduction-band "valleys" with respect to one another and splits the top of the valence band at $\vec{k} = 0$. Carriers in valleys whose energies are raised by strain will transfer to lowered valleys until equilibrium is restored, i.e., until the chemical potential is the same for all valleys. This transfer results in a lower chemical potential in the strained crystal and hence a smaller electronic contribution to the crystal free energy; this means that part of the work spent in deforming the crystal has been regained as a consequence of carrier redistribution, and therefore the effective elastic constant for that strain must decrease. Thus the addition of carriers through doping "softens" the crystal; i.e., it produces a reduction in the shear elastic constants. This effect has been experimentally observed by several authors[3-7] in the second- and third-order elastic constants of $n$- and $p$-type Si and Ge.

A long-wavelength optical vibration of the lattice is in many ways similar to an externally applied stress. The optical phonons, being displacements of sublattices with respect to each other, produce shifts and splittings similar to those produced by shear strains. The symmetry of a $\vec{q} = 0$ optical phonon in the diamond structure is $\Gamma_{25'}$, the same as the symmetry of a traceless [111] strain. Hence the effect of such a phonon on the electronic bands is similar to that of a pure shear [111] strain. Therefore, the long-wavelength optical vibrations of the lattice in a doped semiconductor can also cause a dynamic carrier redistribution among energy bands, which will result in a "softening" of the lattice and thus a decrease in the phonon frequency.

While the effects of free carriers on the elastic constants and on the Raman frequencies are similar, there is, however, an important difference. Measurements of elastic constants are made either under static stress or via strain induced by sound waves of low frequency ($\leq 10^8$ Hz). The redistribution of electrons among valleys can follow the strain at such low frequencies, since, for example, the lowest intervalley scattering rate found by Weinreich *et al.*[8] from acoustoelectrical experiments in very pure Ge is $7\times10^8$ sec$^{-1}$, and greater than $10^{10}$ sec$^{-1}$ in specimens moderately doped with As. Thus the carriers view the perturbation as static, since they redistribute themselves in times much shorter than the period of the perturbation. In our Raman measurements, however, the perturbation has the frequency of the long-wavelength optical phonon, i.e., $\omega_0 \sim 10^{13}$ sec$^{-1}$. The presence of free-carrier effects on $\omega_0$ depends on the ability of carriers to redistribute themselves in a time shorter than the period of $\omega_0$. If $\tau$ is a typical redistribution time, the effect can be observed only if

$$\omega_0 \tau \lesssim 1. \tag{1}$$

Since our $\omega_0$ is very high, in some particular cases Eq. (1) may not be satisfied and the effect will not be observed.

The band edges of semiconductors usually occur at points or lines of high symmetry in the Brillouin zone. Consequently, the electronic contribution to the elastic constants (or Raman frequencies) does not have the most general form permitted by crystal symmetry but has special properties arising from

the symmetry of the band extrema occupied by the carriers. We now discuss the cases of free electrons and holes separately.

### A. Contribution from Free Electrons

The lowest conduction valleys occur along the {111} directions of $\vec{k}$ space at the zone boundary ($L_1$ points) for Ge and along {100} directions ($\Delta_1$ points) near the zone boundary in Si.[9,10] Changes in $C_{44}$ with doping were experimentally observed by Bruner and Keyes[3] in $n$-type Ge. In the present work we sought to find similar changes in the Raman frequency which should be qualitatively related to $C_{44}$.[11] However, no frequency change was found that could be clearly attributed to free-carrier effects. We believe this is caused by the fact that the intervalley scattering time in $n$ Ge is too long and therefore Eq. (1) is not satisfied; i.e., the electrons have no time to redistribute themselves among valleys in one period of oscillation and therefore make no contribution to the $\vec{q} \simeq 0$ optical-phonon frequency. We performed our experiment at temperatures up to 430 °C still with negative results. As a by-product of such observations the temperature dependence of the first-order Raman line in intrinsic Ge was determined; our results are found to be in agreement with Cowley's[12] numerical calculations and with similar measurements for Si by Hart *et al.*[13]

Silicon has its conduction-band valleys along the {100} directions in $\vec{k}$ space inside the Brillouin zone. The $\vec{q} \simeq 0$ optical phonon should not alter the relative positions of these valleys and therefore should produce no electron redistribution among valleys. Hence it seems that there should be no electronic contribution to the Raman frequency or the $C_{44}$ elastic constant in $n$-type Si. However, a small decrease in $C_{44}$ with doping, which can be traced to electronic effects, has been observed.[6,7] We have investigated the dependence of the first-order Raman frequency of $n$-type Si as a function of carrier concentration and found that it decreases systematically as the electron concentration increases; this small effect can be explained as a free-electron contribution. Its origin is explained by the fact that the perturbation splits the $X$-point degeneracy of the conduction band thus producing a lowering in the conduction-band minima quadratic in strain,[14,15] or, in our case, in the amplitude of the phonon vibration. This results in a lowering of the average energy of the free carriers, with the consequent lowering of their contribution to the free energy which, in turn, produces a softening of the lattice [see Fig. 1(b)].

### B. Contribution from Holes

Our perturbation will cause the valence band to split [see Fig. 1(c)] and the dispersion relation of holes to change. The holes will redistribute themselves within and between the light- and heavy-hole bands. This redistribution causes a reduction in all the shear elastic constants ($C_{44}$ and $C_{11}-C_{12}$), as well as in the Raman frequency. Large effects on the elastic constants of $p$-type Si and Ge have been observed.[4,7] A strong dependence of the Raman frequency on hole concentration is reported in this paper.

To study the effect of carriers on the elastic properties of a given semiconductor, a wide range of samples with different carrier concentrations, i.e., dopings, must be used. Therefore, it is essential to separate the effect of electrons or holes on the elastic properties of the material from the effect of the donor or acceptor atoms. This can be done in several ways. First of all, electronic effects produce changes in Raman frequencies and elastic constants which are much larger than direct impurity effects.[1] Also, the free-carrier effects in degenerate semiconductors may be recognized by other features besides their large size; for instance, their effect is insensitive to the species of the impurity and depends exclusively on the carrier concentration. Moreover, free-carrier effects are very sensitive to the symmetry of the band structure. Finally, the free-carrier effects have a characteristic temperature dependence which makes them distinguishable from direct impurity effects.

In Sec. II of this paper, we develop the theoretical

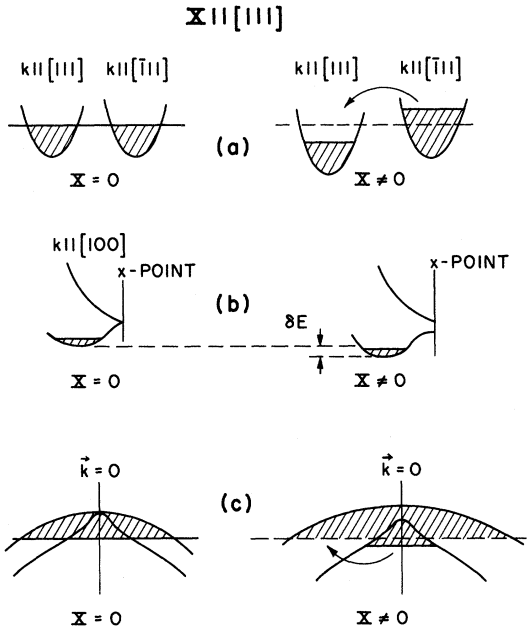


FIG. 1. Illustration of how a $q \simeq 0$ optical phonon, or a traceless [111] strain, affect the energy valleys in the materials of interest: (a) $n$-type Ge, (b) $n$-type Si, (c) $p$-type Si and Ge.

expressions for the frequency shifts of the Raman line as a function of carrier concentration, and the influence of finite electron redistribution times. In Sec. III the experimental details are given. Section IV presents the experimental results and their discussion. Finally, in Sec. V we offer a few concluding remarks.

## II. THEORY

We consider long-wavelength optical vibrations polarized along the [111] axis: Since the cubic symmetry makes all axes equivalent, we choose the polarization which makes the treatment simpler. During vibration, the nearest-neighbor distance $\vec{r}$ changes to

$$\vec{r} = \tfrac{1}{4}a(1+\delta,\ 1+\delta,\ 1+\delta)\ , \tag{2}$$

where $a$ is the lattice constant and $\delta$ represents a deviation from equilibrium. The deformation potential associated with this vibration will be generally designated by $\mathfrak{D}_0$, where $\mathfrak{D}$ is the corresponding deformation potential associated with a pure shear [111] strain; the linear splittings produced by $\mathfrak{D}$ and $\mathfrak{D}_0$ have the same structure. We define $\mathfrak{D}_0$ in such a way that the expressions for the linear splittings under a [111] strain become those under a sublattice shift upon the following substitution:

$$\epsilon\mathfrak{D} \rightarrow \tfrac{1}{8}\mathfrak{D}_0\delta\ , \tag{3}$$

where $\epsilon$ is the off-diagonal component of the strain tensor

$$\overleftrightarrow{\epsilon} = \epsilon \begin{pmatrix} 0 & 1 & 1 \\ 1 & 0 & 1 \\ 1 & 1 & 0 \end{pmatrix} \tag{4}$$

related to the magnitude of the stress $X$ and the compliance constant $S_{44}$ by $\epsilon = \frac{1}{6}XS_{44}$. This definition enables us to decompose the deformation potential $\mathfrak{D}$ into a sum of two terms, one labeled $\mathfrak{D}'$, which would be that produced if the whole unit cell would deform like the macroscopic strain alone, and $-\frac{1}{4}\mathfrak{D}_0\zeta$, the effect of the sublattice displacement associated with the internal strain parameter $\zeta$ of Goroff and Kleinman[16]:

$$\mathfrak{D} = \mathfrak{D}' - \tfrac{1}{4}\mathfrak{D}_0\zeta\ . \tag{5}$$

Equation (5) enables us to extract $\mathfrak{D}_0$ from existing calculations of $\mathfrak{D}$ for several values of $\zeta$.[16,17] We have also obtained algebraic expressions for $\mathfrak{D}_0$ at several points of the bands in terms of pseudopotential form factors[18] (see Appendix A).

We now derive the free energy as a function of $\delta$. If $\vec{r}$ is the nearest-neighbor distance and $\vec{r}_0$ is the same distance in absence of vibrations, the free energy per unit volume can be expanded as follows:

$$F = F_0 + \tfrac{1}{2}[\tfrac{1}{2}N_0\tfrac{1}{2}M\ \omega_0^2(\vec{r}-\vec{r}_0)^2], \tag{6}$$

where $N_0$ is the number of atoms per unit volume, $M$ the atomic mass, $\omega_0$ the frequency of the optical phonons under consideration, and $F_0$ a constant which takes care of other contributions to the free energy. Inserting into Eq. (6) the value of $N_0 = 8/a^3$ ($a$ = lattice constant), and the expression of $\vec{r}-\vec{r}_0$ given in Eq. (2), we finally obtain

$$F = F_0 + \tfrac{3}{2}(M\omega_0^2/8a)\delta^2\ . \tag{7}$$

In order to express Eq. (7) in a form more amenable to comparison with the effect of doping on the elastic constants, we define the quantity

$$C_{44}^* = M\omega_0^2/8a\ , \tag{8}$$

which has the same dimensions and almost the same numerical value[11,19] as the elastic constant $C_{44}$. Equation (7) thus takes the form

$$F = F_0 + \tfrac{3}{2}\ C_{44}^*\ \delta^2\ , \tag{9}$$

which can be immediately compared with the expression of the free energy under a traceless [111] strain:

$$F = F_0 + 6\ C_{44}\epsilon^2\ . \tag{10}$$

Equation (9) transforms into Eq. (10) under the substitutions:

$$C_{44}^* \rightarrow C_{44}, \quad \delta \rightarrow 2\epsilon\ , \tag{11}$$

in agreement with Eq. (3). Equations (9) and (10) must be compared with the expressions for the free-carrier contribution to the free energy in order to assess the changes in $C_{44}$, $C_{44}^*$, and $\omega_0$ with doping.

The free-carrier contribution to the change in free energy per unit volume produced by a deformation is given by[20]

$$\delta F = \sum_k f_k\delta E_k + \frac{1}{2}\sum_k\left(\frac{\partial f_k}{\partial E_k}\right)(\delta E_k)^2\ , \tag{12}$$

where $\delta E_k$ is the change in the carrier energy produced by the deformation (either a stress or a sublattice shift) and $f_k$ is the Fermi distribution. We now consider several cases separately.

### A. Electrons: $n$-Type Ge

This is the multivalley case. The minimum energy of the conduction band occurs along the {111} axes in $\vec{k}$ space at the edge ($L$ point) of the zone. The change in the $C_{44}$ elastic constant with free-carrier concentration was calculated by Keyes[1] to be

$$\frac{\delta C_{44}}{C_{44}} = -\frac{8}{9C_{44}}\ \Phi(\mathcal{E}_2)^2\ , \tag{13}$$

where

$$\Phi = \frac{N}{8k_0T}\ \frac{F'_{1/2}(Z)}{F_{1/2}(Z)}\ , \quad Z = \frac{\mu - E_c}{k_0T}\ .$$

Here $\mu$ is the chemical potential of the unperturbed state, $E_c$ is the energy of the bottom of the unperturbed valley, $F_{1/2}$ are the Fermi integrals,[21] $N$ is the number of carriers per unit volume, and $\mathcal{E}_2$ is the appropriate deformation potential according to the notation of Brooks.[22] Following the prescription of Eqs. (3) and (11), we obtain for Raman frequencies:

$$\frac{\delta C_{44}^*}{C_{44}^*} = 2\frac{\delta\omega}{\omega} = -\frac{8}{9C_{44}^*}\,\Phi\left(\frac{\mathcal{E}_2^0}{4}\right)^2 . \tag{14}$$

We should mention at this point that Eq. (13) does not include changes in $C_{44}$ due to changes in the internal strain parameter $\zeta$ with doping. These changes are discussed in Appendix B.

For the completely degenerate case ($T \to 0$),

$$\Phi = \tfrac{3}{16}(N/\mu) \propto N^{1/3} , \tag{15}$$

and therefore $\delta\omega/\omega$ is proportional to $N^{1/3}$.

### B. Electrons: $n$-Type Si

The lowest conduction-band valleys of Si lie in the $\{100\}$ directions of $\vec{k}$ space, and hence all valleys are equivalent from the point of view of a [111] strain. To first order, a traceless deformation with [111] symmetry leaves the energies of these valleys unaltered. However, the fact that they lie close to the $X$ point in the Brillouin zone [$k = k_0\{100\}$ with $k_0 \simeq 0.86\ (2\pi/a)$, where $a$ is the lattice constant[10]] produces a nonlinear shift due to the stress-induced coupling between the $\Delta_1$ and the $\Delta_{2'}$ conduction bands, related to the $X$-point splitting under a [111] stress. Using the Hamiltonian of Hensel and co-workers,[14] the second-order shift of the $\Delta_1$ conduction-band minima is found to be for a traceless [111] strain[15]:

$$\delta E = -\frac{(2\mathcal{E}_2^*\epsilon)^2}{E(\Delta_{2'}) - E(\Delta_1)} , \tag{16}$$

where $\mathcal{E}_2^*$ is the appropriate deformation potential. Equation (16) represents a uniform lowering of all the valleys which results in a lowering of the energy given by

$$\delta F = -\frac{N(2\mathcal{E}_2^*\epsilon)^2}{E_G} , \tag{17}$$

where $E_G = E(\Delta_{2'}) - E(\Delta_1) \simeq 0.8$ eV at the minimum. As the doping increases, the average $E_G$ decreases and thus an increase in the contribution per carrier to $F$, $\delta F/N$, is expected. However, it is easy to see that this increase should be very small. We can make a power-series expansion of $E_G$:

$$E_G = E_G(0) + A_0(k_x - k_0) + B_0(k_x - k_0)^2 , \tag{18}$$

where $E_G(0)$ is the value of $E_G$ at the minimum ($k_0$) and $k_x$ is the component of $\vec{k}$ along the [100] direction; $k_y$ and $k_z$ do not appear in Eq. (18) because the corresponding masses of the $\Delta_1$ and $\Delta_{2'}$ bands are nearly equal. Equation (16) requires the average of $E_G^{-1}$ for all carriers, e.g.,

$$\left\langle\frac{1}{E_G}\right\rangle = \frac{1}{E_G(0)}\left(1 + \frac{A_0^2\langle(k_x - k_0)^2\rangle}{E_G^2(0)} - \frac{B_0\langle(k_x - k_0)^2\rangle}{E_G(0)}\right) . \tag{19}$$

It is easy to see by looking at the calculated band structure of Si[10] that $B \simeq 0$, therefore,

$$\left\langle\frac{1}{E_G}\right\rangle = \frac{1}{E_G(0)}\left(1 + \frac{A_0^2\langle(k_x - k_0)^2\rangle}{E_G^2(0)}\right) \simeq \frac{1}{E_G(0)}\left(1 + \frac{2A_0^2 m_x}{5E_G(0)}\,\frac{\mu}{E_G(0)}\right) \simeq \frac{1}{E_G(0)}\left(1 + \frac{\mu}{E_G(0)}\right) . \tag{20}$$

The parameters of Eq. (20) (A, $B$, and $m_x$, the effective mass of the $\Delta_1$ conduction band) have been evaluated from the calculated[10] band structure of Si. Equation (20) yields a small increase of the free-carrier contribution to $F$ with increasing doping [$\mu/E_G(0) \leq 0.1$ for our experiments]. A similar argument also leads to an increase in the free-carrier contribution to $F$ with increasing temperature of the order of $k_0T/E_G(0)$. By comparing Eqs. (17) and (20) with Eq. (10), we find

$$\frac{\delta C_{44}}{C_{44}} = -\frac{1}{C_{44}}\,\frac{2}{3E_G(0)}\,(\mathcal{E}_2^*)^2 N\left(1 + \frac{\mu}{E_G(0)}\right) , \tag{21a}$$

where changes in the internal strain parameter with doping have been neglected (see Appendix B). The effect of an optical phonon can be obtained by using the prescription given in Eq. (11),

$$\frac{\delta C_{44}^*}{C_{44}^*} = \frac{2\delta\omega}{\omega} = -\frac{1}{C_{44}^*}\,\frac{2}{3E_G(0)}\left(\frac{\mathcal{E}_{2,0}^*}{4}\right)^2 N\left(1 + \frac{\mu}{E_G(0)}\right) . \tag{21b}$$

### C. Holes: $p$-Type Si and Ge

This situation is not as simple as the previous ones. The valleys under consideration are the top of the doubly degenerate valence bands at $\vec{k} = 0$. These bands are badly warped. Also, the spin-orbit split band interacts with the light-hole band, causing nonparabolicities. Bir and Turnasov[20] made a calculation of the free-carrier-induced shift in the elastic constants which takes into account the warping by averaging it, and entirely neglects the nonparabolicity caused by the spin-orbit-split band. Such a treatment should be only valid for low hole concentrations. In this case the Fermi energy has not yet reached a value close to the spin-orbit splitting $\Delta_0$, at which nonparabolic effects must be taken into account. An estimate based on calculated $\vec{k}\cdot\vec{p}$

bands[10,23] for Ge sets this limit at $\mu \leq \frac{1}{3}\Delta_0$ ($N \leq 3 \times 10^{+19}$ cm$^{-3}$); in the case of Si this limit is reached at even lower carrier concentrations ($N \lesssim 3\times 10^{18}$ cm$^{-3}$) because of the smaller spin-orbit splitting. Bir and Turnasov's[20] expression is

$$\frac{\delta C_{44}}{C_{44}} = -\frac{K m_h}{C_{44}\hbar^2(3\pi^2)^{2/3}}\, d^2 N^{1/3} , \tag{22}$$

where $m_h$ is the heavy-hole mass, $d$ is the appropriate deformation potential, and

$$K = (1+\alpha)^{3/2}\left(\beta + (1-\beta)\frac{(C/B)^2+3}{(C/B)^2+5}\right) . \tag{23}$$

In Eq. (23), $\alpha = m_1/m_h$ and $\beta$, $C$, and $B$ are band parameters defined in Ref. 20. Using Eqs. (3) and (11) we obtain for Raman frequencies

$$\frac{\delta C_{44}^*}{C_{44}^*} = 2\,\frac{\delta\omega}{\omega} = -\frac{K m_h}{C_{44}^*\hbar^2(3\pi^2)^{2/3}}\left(\frac{d_0}{4}\right)^2 N^{1/3} . \tag{24}$$

As already mentioned, Eqs. (22) and (24) are only valid for small hole concentrations ($N < 3\times 10^{19}$ cm$^{-3}$ for Ge and $N < 3\times 10^{18}$ cm$^{-3}$ for Si). Since the concentrations used in our experiment go from $10^{19}$ to $2\times 10^{20}$ cm$^{-3}$, we expect considerable deviations from Eqs. (22) and (24). Similar calculations for intermediate hole concentrations, in which the Fermi energy lies in the nonparabolic region, present considerable difficulties. However, the limit for high carrier concentration, when the Fermi level lies below the nonparabolic region, is quite simple: We can approximate the light- and heavy-hole bands by two parabolic bands (both with masses equal to $m_h$) which run parallel at a constant energy separation of $\frac{2}{3}\Delta_0$. The spin-orbit-split band need not be taken into account because of the small number of carriers which occupy it. The energy shifts with strain of the upper valence bands, far away from $\vec{k}=0$, can be written for the case of a traceless [111] strain, such as that represented by Eq. (4)[24]:

$$\begin{aligned} \delta E &= 0 && \text{for } k \parallel [111] \text{ or } [\bar{1}\bar{1}\bar{1}] \\ &= \pm\frac{8\epsilon^2 d^2}{\Delta_0} && \text{for all other } \{111\} \text{ valleys} \\ &= \pm\frac{9}{2}\frac{\epsilon^2 d^2}{\Delta_0} && \text{for all } \{100\} \text{ valleys} \end{aligned} \tag{25}$$

where the plus and minus signs refer to light- and heavy-hole bands, respectively, and linear terms in strain that average to zero over all directions of $\vec{k}$ have been omitted. We now perform an average of the energy shift over all directions of $\vec{k}$ contained in Eq. (25), and obtain the average shift:

$$\delta E = \pm\tfrac{75}{14}\,(\epsilon^2 d^2/\Delta_0) . \tag{26}$$

We substitute Eq. (26) into Eq. (12) and find

$$\delta F = -\frac{75}{14}\,\frac{\epsilon^2 d^2}{\Delta_0}\,\frac{(2m_h\mu)^{3/2}}{3\pi^2\hbar^3}\left[1-\left(1-\frac{2\Delta_0}{3\mu}\right)^{3/2}\right], \tag{27}$$

under the assumption of degenerate statistics and for $\mu > \frac{2}{3}\Delta_0$. Under the same assumptions, the total number of carriers is given by

$$N = \frac{(2m_h\mu)^{3/2}}{3\pi^2\hbar^3}\left[1+\left(1-\frac{2\Delta_0}{3\mu}\right)^{3/2}\right] + N' , \tag{28}$$

where $N'$ is the number of holes contained in the upper portion of the light-hole band, which has been neglected in this approximation. Using actual $\vec{k}\cdot\vec{p}$ bands[10,23] for Ge, we estimate the value of $N'/N$ to be

$$\frac{N'}{N} \approx 0.1 \quad \text{at } \mu = \tfrac{2}{3}\Delta_0 .$$

This value becomes even smaller as $\mu$ becomes larger than $\frac{2}{3}\Delta_0$ (which is the region of validity of our treatment); we thus make $N'=0$ in Eq. (28). Replacing Eq. (28) in Eq. (27), we get

$$\delta F = -\frac{m_h\gamma_0}{(3\pi^2)^{2/3}\hbar^2}\, d^2(6\epsilon^2)\, N^{1/3} f(x) , \tag{29a}$$

where

$$f(x) = \frac{2^{4/3}}{3x}\,\frac{1-(1-x)^{3/2}}{[1+(1-x)^{3/2}]^{1/3}} , \tag{29b}$$

$$x = 2\Delta_0/3\mu, \quad \gamma_0 = 2^{2/3}\,75/84 = 1.42 . \tag{29c}$$

The function $f(x)$ can be expanded in power series, for $x<1$, as

$$f(x) = 1 - \tfrac{1}{24}\,(x^2+x^3) - \cdots . \tag{30}$$

For $\mu = \Delta_0$ the last term in parens in Eq. (30) contributes less than 2% to $f(x)$ and, therefore, within the limits of our approximation, we set $f(x)=1$ (for $\mu \geq \Delta_0$). With this in mind we compare Eq. (29a) to Eq. (10) and obtain for the free-carrier contribution to $C_{44}$

$$\frac{\delta C_{44}}{C_{44}} = -\frac{m_h\gamma_0}{(3\pi^2)^{2/3}\hbar^2}\,\frac{d^2}{C_{44}}\, N^{1/3} \quad (\mu > \Delta_0) . \tag{31}$$

The effect of a $\vec{q}=0$ optical phonon can be obtained using Eq. (11):

$$\frac{\delta C_{44}^*}{C_{44}^*} = 2\,\frac{\delta\omega}{\omega} = -\frac{m_h\gamma_0}{(3\pi^2)^{2/3}\hbar^2}\,\frac{1}{C_{44}^*}\left(\frac{d_0}{4}\right)^2 N^{1/3} . \tag{32}$$

We now have expressions that are valid in the low [Eq. (24) for $\mu < \frac{1}{3}\Delta_0$] and the high [Eq. (32) for $\mu > \Delta_0$] carrier concentration limits.

### D. Redistribution Time

So far we have derived the Raman frequency shifts produced by free carriers considering a static sublattice displacement; i.e., in our derivation

it was implicitly assumed that carriers are in thermal equilibrium at all times while the lattice vibrates. Actually, an optical phonon is a rapidly varying sublattice displacement with a frequency $\omega_0 \simeq 10^{13}$ sec$^{-1}$. The previous derivations are valid only if $\omega_0\tau \ll 1$, where $\tau$ is the mean time in which the carriers redistribute themselves into thermal equilibrium. On the other hand, if $\omega_0\tau \gg 1$, no effect can be observed; the carriers do not have time to redistribute themselves between oscillations and hence do not contribute to the change in free energy. In the case where $\omega_0\tau \simeq 1$, a frequency shift will still be present, but the results of the previous sections have to be modified to take into account the fact that all carriers do not redistribute themselves into equilibrium (the frequency shift should be smaller). Also, a "time lag" will exist between the oscillation of the lattice and the redistribution of carriers: The Raman peak will broaden. To put this notion on a quantitative basis, let us call $F_0$ the free energy in the absence of the vibration, $F_s$ the free energy in the presence of a static sublattice displacement, and $F$ the free energy in the presence of a lattice vibration of frequency $\omega_0$. The change in free energy for a static sublattice displacement is the quantity already computed in previous sections:

$$\delta F_s = F_s - F_0 = -\tfrac{1}{2} C_0\, \delta^2 , \tag{33}$$

where $C_0$ is a constant whose value has already been computed for all the cases of interest, and $\delta$ is the normalized sublattice displacement introduced in Eq. (2). In the dynamic case, $\delta = \delta_0 e^{i\omega_0 t}$ and $F \sim e^{2i\omega_0 t}$. Now, $F$ will fall short of the static value $F_s$, as we mentioned previously. In fact, $F - F_s$ will contain an oscillatory term, coming from substitution in Eq. (33) of $\delta$ by its dynamic counterpart, and an exponentially decaying factor due to the finite redistribution time, i.e.,

$$\frac{d}{dt}(F - F_s) = -\frac{1}{\tau}(F - F_s) + \frac{1}{2} C_0 \frac{d}{dt}(\delta^2) . \tag{34}$$

Replacing $\delta \sim e^{i\omega_0 t}$ in Eq. (34), we find

$$2i\omega_0 (F - F_s) = -(1/\tau)(F - F_s) + i\omega_0 C_0 \delta^2 .$$

Noticing that

$$\delta F = F - F_0 = F - F_s + F_s - F_0 ,$$

and using Eq. (33), we find

$$\delta F = \delta F_s / (1 + 2i\omega_0\tau) . \tag{35}$$

Since $\delta F \sim \delta\omega$ and $\delta F_s \sim \delta\omega_s$, where $\delta\omega$ and $\delta\omega_s$ are the frequency shifts in the dynamic and static cases, respectively, we obtain

$$\delta\omega = \delta\omega_s / (1 + 2i\omega_0\tau) . \tag{36}$$

Thus, the dynamic frequency shift is smaller than the static one and has an imaginary part that should appear as a broadening of the Raman line ($\Gamma$):

$$\delta\omega_r = \frac{\delta\omega_s}{1 + (2\omega_0\tau)^2} , \quad \delta\omega_i = \Gamma = \frac{\delta\omega_s (2\omega_0\tau)}{1 + (2\omega_0\tau)^2} , \tag{37}$$

where the subindices $r$ and $i$ stand for the real and imaginary part of the dynamic frequency shift, respectively. For $\tau \to 0$, the frequency shift $\delta\omega_r$ equals the static one $\delta\omega_s$, and $\Gamma = 0$. For $\tau \to \infty$, both $\delta\omega$ and $\Gamma$ vanish, $\delta\omega$ more rapidly than $\Gamma$. There is a broad range $2\omega_0\tau \simeq 1$ in which the frequency shift is considerably reduced by the redistribution time and a substantial broadening ($\Gamma$ is maximum for $2\omega_0\tau = 1$) should occur.

### E. Direct Impurity Effects

We have so far discussed the free carrier contributions to the frequency shifts produced by doping. Actually, the phonon frequency may be affected by the presence of the impurity itself. In this section we estimate the size of such an effect in order to be able to distinguish between purely electronic and purely impurity-induced frequency shifts.

Perhaps the simplest way in which an impurity can affect the phonon frequency is through a change in the "average" atomic mass, which enters the frequency as $\omega \propto M^{-1/2}$, and a change in the "average" volume, which should affect the frequency through the Grüneisen parameter. The changes in average mass and average volume are

$$\bar{M} = M(1 - a_M \eta) , \quad \bar{V} = V(1 - 3a_v \eta) , \tag{38}$$

where $\bar{M}$ and $\bar{V}$ are the average atomic mass and volume, respectively, $M$ and $V$ the atomic mass and volume of the pure semiconductor, and $\eta$ the fractional impurity concentration. The parameters $a_M$ and $a_V$ are defined as

$$a_M = (M - M_I)/M , \quad a_V = (\rho - \rho_I)/\rho , \tag{39}$$

where $M_I$ is the atomic mass of the impurity atom and $\rho$ and $\rho_I$ are the covalent radii[25] of the host and impurity atom, respectively. From the dependence of the frequency on mass and from the definition of the Grüneisen parameter, it is possible to write

$$\frac{\delta\omega_0}{\omega_0} \simeq -\frac{1}{2}\frac{\delta\bar{M}}{M} , \quad \gamma = -\frac{V}{\omega_0}\frac{d\omega_0}{dV} ,$$

and thus we find for the frequency shifts induced by the impurities the approximate expression

$$\frac{\delta\omega_0}{\omega_0} \simeq (\tfrac{1}{2} a_M + 3\gamma a_V)\eta . \tag{40}$$

## III. EXPERIMENT

Our measurements were performed with the 4880-Å line of a $\frac{1}{2}$-W argon-ion laser (Coherent Radiation, model No. 54) in the backscattering configuration. A Jarrell-Ash 1-m monochromator with detection

by photon counting was used. The wavelengths of the phonon-shifted lines were determined by comparison with several reference lines of a neon low-pressure lamp.

The low-temperature measurements were performed with the samples immersed in liquid nitrogen. The high-temperature measurements were performed in an evacuated glass Dewar with the sample held in mechanical contact with a heated copper block. The temperature was monitored with a copper-constantan thermocouple placed near the sample. The temperature stability was better than $\pm 1\,^{\circ}\mathrm{C}$.

The samples were cut from single crystals, mechanically polished, and etched with a CP-4 solution. The carrier concentration was ascertained by Hall-effect and electrical conductivity measurements.

## IV. RESULTS AND DISCUSSION

We have observed the first-order Raman peaks of $n$- and $p$-type Si and Ge with various carrier concentrations. The results can best be discussed for each group of materials separately.

### A. Holes: $p$-Type Si and Ge

The Raman spectrum of $p$-type Si and Ge was studied for a variety of hole concentrations at room and liquid-nitrogen temperatures. In Figs. 2–5 we show the spectra of some typical samples of these materials. As we increase the carrier concentration, the peaks exhibit a marked decrease in frequency and a considerable broadening. As we go from room temperature to liquid-nitrogen temperature, the frequency shifts for the lower concentration samples decrease while the broadening of the peaks remains unchanged. This effect is demonstrated in Figs. 4 and 5, where the Si sample with $p \simeq 1\times 10^{19}$ cm$^{-3}$ has a finite frequency shift at room temperature but none at liquid-nitrogen temperature. This fact suggests that the hole-redistribution time is in the region $2\omega_0\tau \simeq 1$, for which the

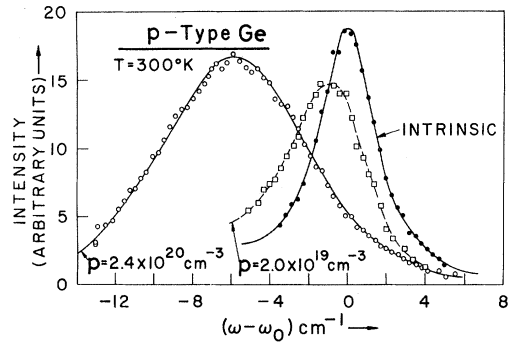


FIG. 2. Raman spectra of several typical $p$-type Ge samples at room temperature.

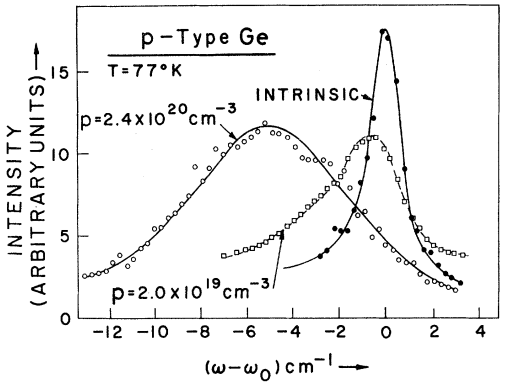


FIG. 3. Raman spectra of several typical $p$-type Ge samples at $T = 77\,^{\circ}\mathrm{K}$.

broadening is maximum (see Sec. IIC). It also indicates that direct impurity effects are not dominant, and that the observed effects are of electronic nature, since a direct impurity effect such as estimated in Sec. IIE would be temperature independent. Let us compare the order of magnitude of the observed effects with those estimated as direct impurity effects with the expressions derived in Sec. IIE. We rewrite Eq. (40) in the following way, making use of the fact that the Grüneisen parameter for Si and Ge is approximately one[26]:

$$Y_I = (\tfrac{1}{2}a_M + 3a_V)\,QX\,, \tag{41}$$

where

$$X = 10^{-19}N \quad (N \text{ in cm}^{-3}), \quad \eta = 10^{-3}\,QX,$$
$$Q = \begin{cases} 0.24 & \text{for Ge} \\ 0.20 & \text{for Si}\,, \end{cases} \tag{42}$$
$$Y = 10^3(\delta\omega/\omega) \quad \text{(frequency shift in parts per thousand)}.$$

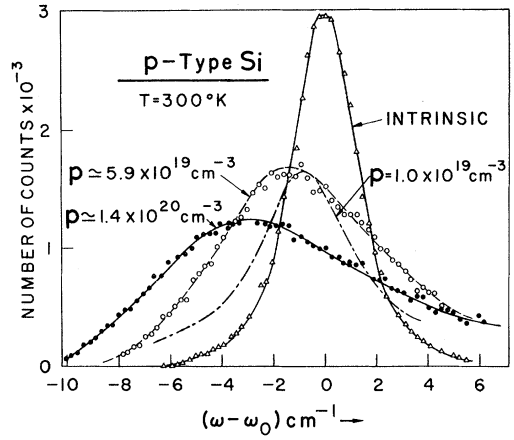


FIG. 4. Raman spectra of several typical $p$-type Si samples at room temperature.

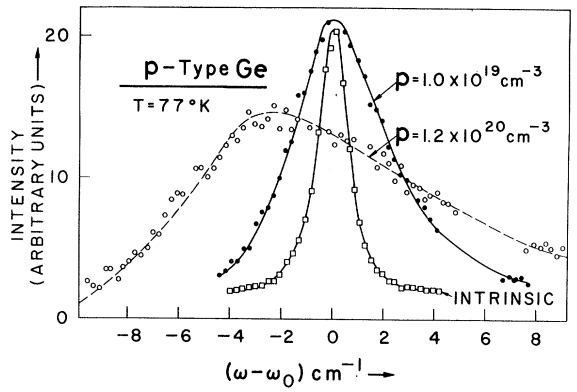


FIG. 5. Raman spectra of several typical $p$-type Si samples at $T=77\,^{\circ}\mathrm{K}$.

TABLE I. Comparison of estimated impurity shifts and observed frequency shifts for a given hole concentration in $p$-type Si and Ge.

| Material | $X=10^{-19}N$ ($cm^{-3}$) | $10^3\eta$ (impurity concentration in parts per thousand) | $a_M$ | $a_V$[a] | $Y_I$ | $Y$ (expt.) |
|---|---|---|---|---|---|---|
| Ge (Ga doped) | 24 | 5.8 | 0.037 | 0 | 0.1 | −20 |
| Si (B doped) | 14 | 2.8 | 0.64 | 0.20 | 2 | −6 |

[a]Calculated from the covalent radii given in Ref. 31.

The Ge samples were doped with Ga, and the Si samples were doped with boron. The relevant parameters for using Eq. (41) are listed on Table I, as well as the predictions of Eq. (41) compared to the observed shifts. We see from Table I that the observed shifts are much larger and of opposite sign to those predicted on the basis of impurity effects; this fact, coupled with the temperature dependence of frequency shifts and peak broadenings, indicates that the dominant mechanism for the shift is electronic.

We now try to correlate the experimental results with the expressions derived in Sec. II C and the parameters of Table II. We can rewrite the results for high and low carrier concentrations [Eqs. (24) and (32)] as

$$Y=-bX^{1/3} \quad (\mu<\tfrac{1}{3}\Delta_0)$$
$$=-\left(\frac{\gamma_0}{K}\right)bX^{1/3} \quad (\mu>\Delta_0)\,, \tag{43}$$

where

$$b=\frac{10^{19}Km_h(10)^{1/3}}{\hbar^2(3\pi^2)^{2/3}C_{44}^*}\left(\frac{d_0}{4}\right)^2\,, \tag{44}$$

and $\gamma_0=1.42$. In Figs. 6 and 7 a logarithmic plot of frequency shifts versus carrier concentration is shown; the experimental points are compared with the straight lines obtained from Eq. (43):

$$\log_{10}|Y|=\log_{10}b+\tfrac{1}{3}\log_{10}X \quad (\mu<\tfrac{1}{3}\Delta_0)$$

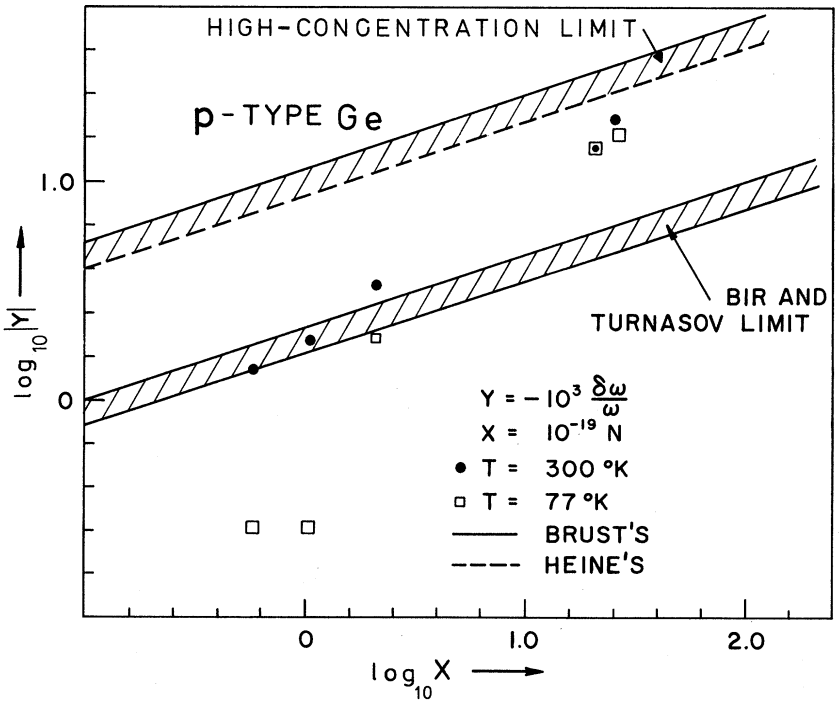


FIG. 6. Logarithmic plot of observed frequency shifts in parts per thousand for $p$-type Ge vs carrier concentration (at room and liquid-nitrogen temperatures). Solid lines calculated with Brust's pseudopotentials; dashed lines with Heine's pseudopotentials.

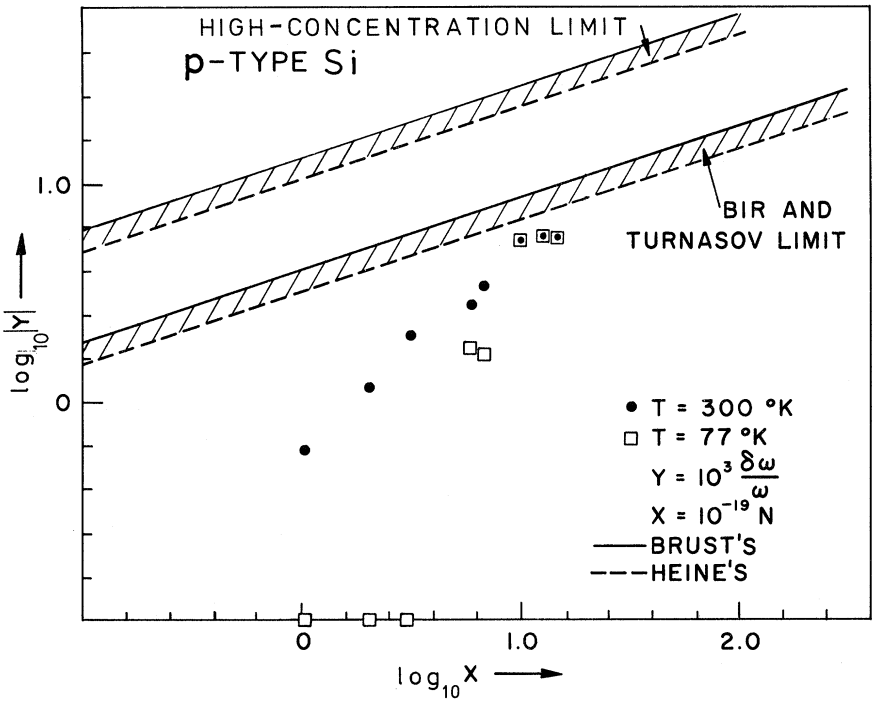


FIG. 7. Logarithmic plot of observed frequency shifts in parts per thousand for $p$-type Si vs carrier concentration (at room and liquid-nitrogen temperatures). Solid lines calculated with Brust's pseudopotentials; dashed lines with Heine's pseudopotentials.

$$= \log_{10}(\gamma_0/K) + \log_{10} b + \tfrac{1}{3}\log_{10} X \quad (\mu > \Delta_0). \qquad (45)$$

Although the experimental points for Ge at room temperature fall between the two asymptotic limits predicted by Eq. (45), for Si the experimental points, at room temperature, fall below the lowest line. At liquid-nitrogen temperature the points fall below the room-temperature points, especially at low carrier concentration. We believe this is a redistribution time effect. Equation (45) gives the theoretical limit for $\tau \to 0$ (static sublattice shift); what we measure, however, is the dynamic frequency shift given by Eq. (37):

$$Y' = Y/[1 + (2\omega_0\tau)^2], \qquad (46)$$

where $Y'$ is the measured quantity, and $Y$ is the quantity given by Eq. (45). The existence of a finite relaxation time makes the measured frequency shift smaller than the one predicted by Eq. (45). The temperature dependence is understood when one considers that for low impurity concentrations the relaxation time is dominated by phonon scattering (thus $\tau$ decreases markedly with increasing temperature), and for high impurity concentrations the relaxation time is dominated by impurity scattering (thus rendering $\tau$ temperature independent). For

TABLE II. Parameters that enter into the calculation of the frequency shifts for $p$-type Si and Ge.

| Material | $C_{44}^{*}$[a] ($10^{11}$ dyn/cm$^2$) | $C_{44}$[a] ($10^{11}$ dyn/cm$^2$) | $\frac{1}{4}d_0$ (eV)[b] | $b$ (cm) |
|---|---|---|---|---|
| Ge | 9.2 | 6.71 | 8.3–7.36 | 2.16–1.68 |
| Si | 10.6 | 7.96 | 8.4–7.25 | 4.16–3.30 |

[a]Reference 20. [b]From Appendix A.

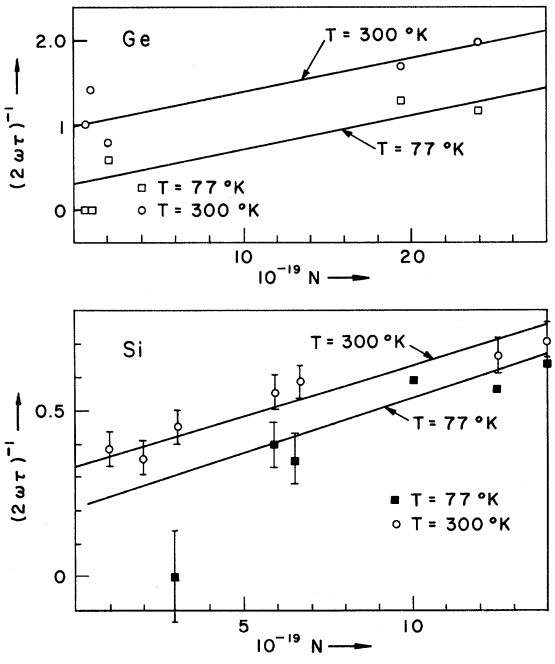


FIG. 8. Inverse scattering times $(2\omega_0\tau)^{-1}$ obtained from linewidths as a function of carrier concentration.

TABLE III. Comparison of the relaxation times obtained from our room-temperature experimental linewidths with relaxation times from the electrical conductivity.

| Material | Phonon scattering $\omega_0\tau$ (our expt.) | Phonon scattering $\omega_0\tau$[a] (conductivity) | Impurity scattering ($N=2\times10^{20}$ cm$^{-3}$) $\omega_0\tau$ (our expt.) | Impurity scattering ($N=2\times10^{20}$ cm$^{-3}$) $\omega_0\tau$ (conductivity) |
|---|---|---|---|---|
| Ge | 0.5 | 0.35 | 0.3 | 0.3[b] |
| Si | 1.5 | 0.5 | 0.6 | 0.3[c] |

[a]C. Kittel, *Introduction to Solid State Physics*, 3rd ed. (Wiley, New York, 1967), p. 308.
[b]J. C. Irvin, Bell System Tech. J. 41, 387 (1962).
[c]S. M. Sze, *Physics of Semiconductors* (Wiley-Interscience, New York, 1969), p. 43.

low concentrations, when we decrease the temperature there is a marked increase in $\tau$: The observed frequency shift becomes smaller. For higher impurity concentrations, however, $\tau$ and thus the frequency shift, is practically independent of temperature. It is possible to estimate $\tau$ from the observed width of the Raman line. If we assume a Lorentzian line shape and we call the width of a given peak $W$ (full width at half-power), and the width of the peak corresponding to the intrinsic material $W_0$, we have, using Eq. (37),

$$\tfrac{1}{2}(W-W_0)=\Gamma=\frac{(2\omega_0\tau)\delta\omega_s}{1+(2\omega_0\tau)^2}\,,\quad \delta\omega_r=\frac{\delta\omega_s}{1+(2\omega_0\tau)^2}\,, \tag{47}$$

where the widths $W$ and $W_0$ were corrected for instrumental resolution in the way specified in Sec. IV C. From Eq. (47) the ratio of the observed change in width to the observed frequency shift gives an estimate of the relaxation time:

$$(W-W_0)/2\delta\omega_r=2\omega_0\tau\,. \tag{48}$$

In Fig. 8 we show a plot of $\tau^{-1}$ computed with Eq. (48) versus carrier concentration. It seems that $\tau^{-1}$ increases roughly linearly as the carrier concentration increases. The use of Eq. (48) with the experimental data at room temperature for the lowest carrier concentration should give us the relaxation time of the phonon scattering process alone and for higher $N$ the relaxation time for impurity scattering. In Table III we list these two limits calculated from our experimental linewidths and compare them with relaxation times obtained from conductivity measurements at room temperature. However, we must keep in mind that $\tau$ is the time for scattering from the light-hole to the heavy-hole band. In the low-doping region, where $\tau$ is mostly determined by phonon scattering, it is easy to obtain $\tau$ from the conductivity $\sigma$ by remembering that the scattering between two states in the light-hole band has the same probability as the scattering from a state in the light-hole band to a state in the heavy-hole band.[22] One thus obtains

$$\tau=(\sigma/Ne^2)\,[m_l^{3/2}/(m_h^{1/2}+m_l^{1/2})]\,. \tag{49}$$

The temperature dependence of $\sigma$ also explains

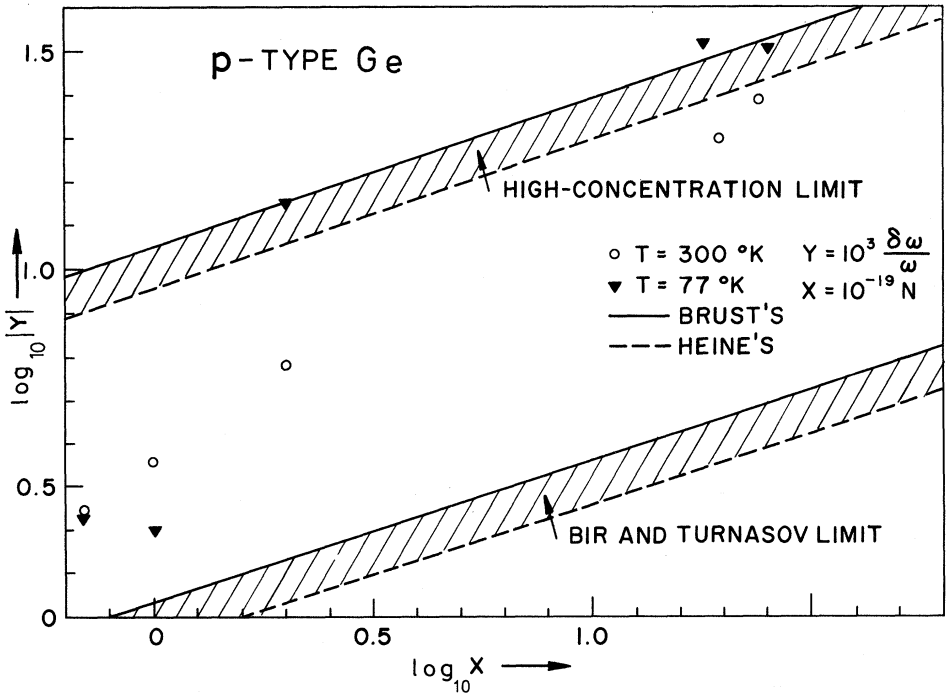


FIG. 9. Logarithmic plot of frequency shifts in parts per thousand, corrected for scattering time effects, for $p$-type Ge vs carrier concentration.

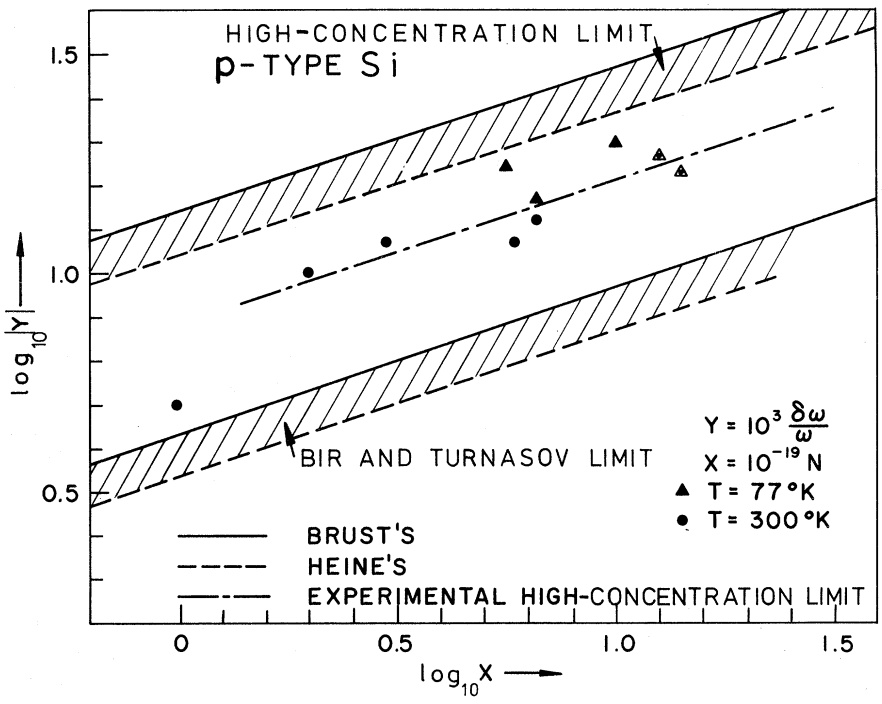


FIG. 10. Logarithmic plot of frequency shifts in parts per thousand, corrected for scattering time effects for $p$-type Si vs carrier concentration. Solid lines calculated with Brust's pseudopotentials; dashed lines with Heine's pseudopotentials.

through Eq. (49) the observed change in $\omega_0\tau$ between room and liquid-nitrogen temperature. In this case it is difficult to extract quantitative estimates of $\omega_0\tau$ from our data, since no frequency shift was observed for the lowest carrier concentrations. Setting the minimum observable frequency shift at one-twentieth of the linewidth, however, we get a lower limit for $\omega_0\tau$ at $T = 77\,^{\circ}\mathrm{K}$: $\omega_0\tau > 10$. The values predicted by Eq. (49) are $\omega_0\tau = 30$ for Si and $\omega_0\tau = 21$ for Ge in agreement with these findings.

The redistribution time $\tau$ for the heavy doped, impurity scattering controlled case is more difficult to handle because of the lack of an appropriate scattering theory. Therefore, we take for the relationship between $\sigma$ and $\tau$: $\tau = \sigma/Ne^2$, which should be accurate to within a factor of the order of 1.

Having calculated the relaxation time from the linewidths, we can substitute this time into Eq. (46) to compute $Y$ (static frequency shift in parts per thousand), which may then be compared with the prediction of Eqs. (45). In Figs. 9 and 10 we plot again logarithmically the static frequency shifts $Y$ (circles and triangles) versus carrier concentration, and we compare these points with the asymptotic behavior predicted by Eq. (45) (solid lines). The agreement is quite good. We can now use the experimental points as means of determining a value for the deformation potential $d_0$ and compare this value with the theoretical estimates (see Appendix A) used in Eqs. (45) to obtain the solid lines in Figs. 9 and 10. This comparison, shown in Table IV, is satisfactory.

### B. Electrons: $n$-Type Si

We have seen in Sec. IIB that the {100} conduction-band valleys of Si do not shift in energy with respect to one another under a traceless [111] deformation. There is, however, an over-all quadratic lowering of these valleys that could account for the small electronic effect in $C_{44}$ reported by Hall[6] and by Beilin *et al.*,[7] and the small changes in Raman frequencies reported in this work. Inserting into Eqs. (29) the parameters listed in Table V, we find

$$10^3(\delta C_{44}/C_{44}) = -0.95\,X(1+0.02X^{2/3})\,,$$
$$Y = 10^3(\delta\omega/\omega) = -0.025\,X(1+0.02X^{2/3}), \tag{50}$$

In Table VI we show a comparison of the experimental results for $C_{44}$ and the Raman frequency (the last for only one concentration) at room and

TABLE IV. Comparison of deformation potentials obtained from our experiment with the theoretical estimates of Appendix A.

| Material | $\frac{1}{4}d_0$ (theoret.) (eV) | $\frac{1}{4}d_0$ [a] (theoret.) (eV) | $\frac{1}{4}d_0$ [b] (expt.) (eV) |
|---|---|---|---|
| Ge | 7.25 | 8.3 | 7.25 |
| Si | 6.1 | 8.4 | 7.25 |

[a] From Appendix A, using the pseudopotential form factors of Ref. 35.

[b] From Appendix A, using the pseudopotential form factors of Ref. 36.

TABLE V. Parameters that enter into the calculation of frequency shifts for $n$-type Si.

| $\mathcal{E}_2^*$ [a] | $\mathcal{E}_{2,0}^*$ [b] | $\mathcal{E}_{2,0}^*$ [c] | $E_G(0)$ [d] (eV) | $m_\parallel$ [d] (units of $m_0$) | $m_\perp$ [e] (units of $m_0$) |
|---|---|---|---|---|---|
| 7.5±2 | 2.02 | 1.97 | 0.8 | 0.916 | 0.190 |

[a]Reference 14.
[b]Appendix A, with pseudopotential form factors from Ref. 35.
[c]Appendix A, with pseudopotential form factors from Ref. 36.
[d]Reference 10.
[e]Reference 13.

low temperatures, with the predictions of Eqs. (50). We see that there is a reasonable agreement between the predictions of Eq. (50) and the experimental values of $C_{44}$ determined by Hall[6] at low temperatures. The predicted changes are smaller than the experimental ones for the Raman frequencies and also for the elastic constant measured by Beilin *et al.*[7] We also notice that Hall's measurements and our measurements show a small increase of $\delta\omega_0$ and $\delta C_{44}$ with temperature, in accordance with Sec. IIB. Beilin *et al.* observe an anomalous temperature dependence which they try to justify theoretically; however, their derivation of the change in $C_{44}$ [Eq. (5) of Ref. 7] seems to be in error.

We measured the Raman frequency of $n$-type Si for several carrier concentrations. To facilitate comparison between theory and experiment, we recast Eq. (50) into the following form

$$Y' = \frac{-Y}{(1+0.02X^{2/3})} = 0.025X\ . \tag{51}$$

In Fig. 11 we have plotted the values of $Y'$ obtained from our data (circles) as a function of carrier concentration. From this figure we infer a dependence

$$Y' = (0.09 \pm 0.03)X\ , \tag{52}$$

with a larger slope than that predicted by Eq. (51). The difference can be accounted for as an inaccuracy in the theoretical deformation potential (see Appendix A) used in the evaluation of Eq. (51). If we use the data of Fig. 11 for an experimental estimate of the deformation potential, we obtain $\mathcal{E}_{2,0}^* = (3.8 \pm 1.3)$ eV, which is less than double the theoretical estimate $\mathcal{E}_{2,0}^* = 2$ eV. Because of the approximations involved, and the existence of large cancelling terms in the estimate of $\mathcal{E}_{2,0}^*$, such an error is not unacceptable.

In our experiments we have used samples doped with both As and P. The mass and size effects predicted by Eq. (56) are

$$Y' = 0.16X \text{ for As}$$

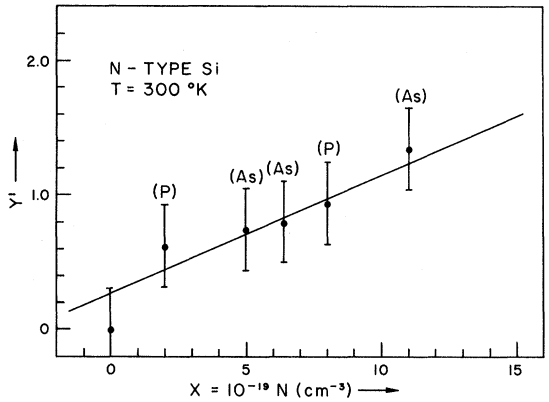


FIG. 11. Frequency shifts in parts per thousand, divided by the factor $[1+\mu/E_G(0)]$ of Eq. (67) vs carrier concentration for $n$-type Si at room temperature.

$$= 0.01X \text{ for P}\ . \tag{53}$$

Therefore, while impurity effects should be large for As-doped samples, they should be negligible for the P-doped ones; however, we see in Fig. 11 that no difference is apparent between phosphorous- and arsenic-doped samples (the dopant is shown above each point). Thus the only parameter of importance in determining the frequency shift seems to be the carrier concentration. We may therefore conclude that the effects we have seen are electronic, of the type described by Eq. (51). The question remains of why Eq. (53) overestimates the mass and size effects. This equation was obtained under the assumption of an average mass and an average lattice constant, which may give an overestimate of the effect. The perturbation of the phonon spectrum produced by the heavier impurities is likely to be concentrated in the vicinity of some local or resonance modes, and thus at the top of the phonon spectrum ($\omega_0$) may be smaller than predicted by Eq. (53).

TABLE VI. Comparison of experimental results for elastic constants and Raman frequencies with our theoretical predictions.

| $X$ | | From Eq. (66) | Expt. Room temp. ($T=300$ °K) | Expt. Low temp. |
|---|---|---|---|---|
| 4.8 | $10^3\frac{\delta C_{44}}{C_{44}}$ Beilin *et al.* (Ref. 7) | −4±2 | −10 | −15 ($T=77$ °K) |
| 2.0 | $10^3\frac{\delta C_{44}}{C_{44}}$ Hall (Ref. 6) | −2±1 | −4.1±0.4 | −3.4±0.3 ($T=4.2$ °K) |
| 6.4 | $10^3\frac{\delta\omega}{\omega}$ (our expt.) | −0.2 | −(0.85±0.2) | −(0.53±0.2) ($T=77$ °K) |

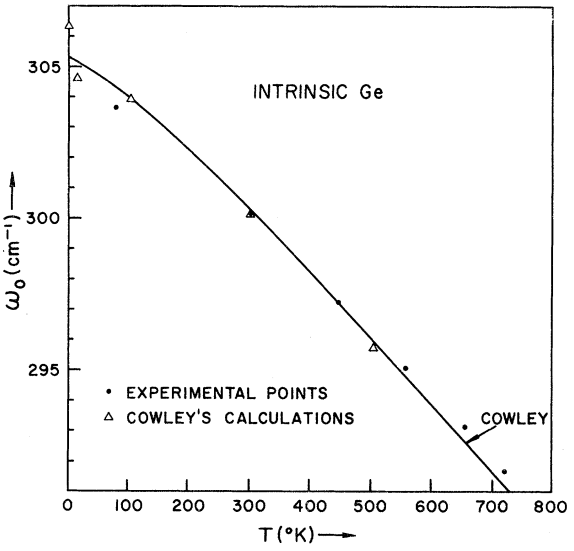


FIG. 12. Frequency of the $q \simeq 0$ optical phonon in intrinsic Ge as a function of absolute temperature. The circles are our experimental data and the triangles Cowley's predictions. The solid line was drawn through Cowley's points.

As a final comment, we indicate that no broadening of the Raman line with doping was observed in $n$-type Si, thus implying $\omega_0\tau \ll 1$. Therefore, it is unnecessary to perform any scattering time corrections when analyzing the frequency shifts.

### C. Electrons: $n$-Type Ge

In this case we have been unable to detect any shift in the Raman frequency that can be attributed to electronic effects. The shifts observed are too small and seem to depend critically on the nature of the dopant, rather than on the carrier concentration. In fact, for one As-doped sample ($T = 300\,^\circ$K, $N = 4.8 \times 10^{19}$ cm$^{-3}$), we find a small decrease in the phonon frequency (of the order of 0.2% as compared with shifts of the order of 1% for $p$-type Ge of the same carrier concentration), while for a P-doped sample of the same carrier concentration there is an increase in the phonon frequency of the order of 0.1%. Since the electronic effects in $C_{44}$ have been observed by Bruner and Keyes,[3] we conclude that the nonexistence of a similar effect for the Raman frequency is due to the long intervalley scattering time of the conduction electrons of Ge. This conclusion is supported by the fact that intervalley scattering times for moderately doped Ge are of the order of $10^{-10}$ sec.[8] This makes $\omega_0\tau \simeq 10^3$ which, when inserted into Eq. (37), gives a dynamical frequency shift $10^{-6}$ times smaller than that predicted by the static theory; such small shifts are undetectable. The measurements were also carried out at high temperatures with still negative results.

While performing the experiment at different temperatures, we measured the temperature dependence of the Raman line for intrinsic Ge. In Fig. 12 these results are compared with the theoretical predictions of Cowley.[12] The agreement between Cowley's theory (solid line drawn between Cowley's numerical values given as triangles) and our experiment (circles) is excellent. Similar results have been recently reported by Ray *et al.*[27]

Next, the linewidths (full width at half-maximum) are analyzed as a function of temperature. It becomes necessary, especially at low temperatures, to correct the observed linewidth for the instrumental resolution by extrapolation to zero spectral slit width. The correction is made, under the assumption of Gaussian slit functions and line shapes, with the expression

$$W(\text{observed}) = (W^2 + W_I^2)^{1/2}, \tag{54}$$

where $W$ is the corrected linewidth and $W_I$ the instrumental resolution ($W_I = 1.7$ cm$^{-1}$ for a slit width of 50 $\mu$ measured with the laser line).

It has been suggested[13] that the linewidth of the Raman line is determined mostly by decay into two LA phonons of half-energy, and hence its temperature dependence is

$$W(T) = W(0)\,[1 + (e^{\hbar\omega_0/k_0T} - 1)^{-1}]\,. \tag{55}$$

Figure 13 shows excellent agreement between the corrected linewidths, the predictions of Eq. (55) (solid line), and Cowley's more complete theoretical calculations.

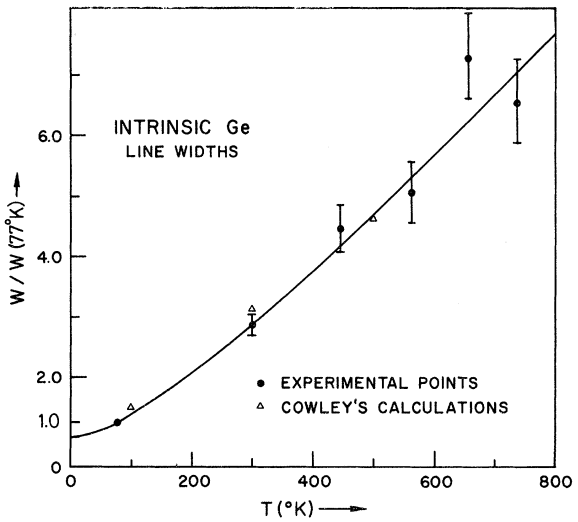


FIG. 13. Linewidths of the Raman line for intrinsic Ge, normalized to $W(77)$, as a function of absolute temperature. The circles are our experimental data and the triangles Cowley's calculated values. The solid line is calculated with Eq. (71).

## V. CONCLUSIONS

We have measured the lowering of the Raman frequency of Ge and Si induced by heavy free-carrier concentrations. The effect observed agrees reasonably with the predictions of deformation-potential theory. The shifts are limited by the time it takes the carriers in the split bands to reach thermal equilibrium. The long intervalley scattering time completely suppresses the effect in $n$-type Ge, while the much shorter scattering time only decreases the effect slightly at low carrier concentrations in the $p$-type materials. Some extensions of the present work suggest themselves. Application of uniaxial stress along the appropriate direction can shift all carriers into one valley: Strong changes in the effects of doping on the Raman frequency and on the elastic constants are expected. This work should help to separate electronic effects from ionic mass and size effects. A [100] stress would also increase the free-carrier effect in $n$-type Si by raising the Fermi level [see Eq. (20)]. The direct effects of the stress on the phonon spectrum of the pure material are well understood and could be easily taken into account.[28,29]

We have also found that there should be an effect of the high free-carrier concentration on the internal strain parameter $\zeta$ ($\zeta$ decreases with doping). In $p$-type materials this should be quite substantial and may be directly measurable with x-ray scattering.[30] This change in $\zeta$ produces a second-order change in $C_{44}$ which is too small to be detected experimentally.

### ACKNOWLEDGMENTS

We would like to thank Professor H. Maris for innumerable discussions and Dr. C. J. Buchenauer for his help with the Raman equipment.

### APPENDIX A

Using a pseudopotential approach we have computed the values of the deformation potentials $\mathfrak{D}_0$ for a sublattice displacement (optical vibration) at several symmetry points of the Brillouin zone of diamond-type semiconductors.[19] The expressions for the deformation potential $d_0$ of the $\Gamma_{25'}$ valence band are

$$\frac{d_0}{4}=\frac{\pi}{\sqrt{3}}\,\frac{(v_3-v_{11})^2}{E_2}\left(1-\frac{v_4-v_{12}}{E_2-\frac{1}{2}(\epsilon_0+v_8)}\right), \tag{A1}$$

where

$$E_2=\{[\tfrac{1}{2}(\epsilon_0+v_8)]^2+2(v_3-v_{11})^2\}^{1/2}, \qquad \epsilon_0=(\hbar^2/2m_0)(2\pi/a)^2 . \tag{A2}$$

The $v_k$'s are the atomic pseudopotential form factors for a vector $\vec{k}$ of magnitude $k$. Equation (A1) yields for Si and Ge the values listed in Table IV. Two values of $d_0$ have been calculated, using either the $v_k$'s of Brust[31] or those of Animalu and Heine.[32]

For the $X_1$ conduction band in Si, the appropriate deformation potential is, in the approximation of Heine and Jones,[33]

$$\tfrac{1}{4}\mathcal{E}^*_{2,0}=\frac{\pi}{4}\left(v_4+\frac{4v_3-(\epsilon_0+v_8)^2v_4}{4E_3}\right), \tag{A3}$$

with

$$E_3=\{[\tfrac{1}{2}(\epsilon_0+v_8)]^2+2v_3^2\}^{1/2} . \tag{A4}$$

The values obtained with Eq. (A3) for Si, using Brust's[31] and Animalu and Heine's[32] pseudopotential form factors, are listed in Table V.

### APPENDIX B

We have mentioned in Sec. II that doping may alter the internal strain parameter $\zeta$ for [111] stress. This change in $\zeta$ may, in turn, produce changes in $C_{44}$, in addition to those of Eqs. (22b), (29a), and (40b). We use the bond-stretching–bond-bending model of Martin,[19] which accounts well for the experimental value of $\zeta$ in pure Ge and Si. Let $\alpha$ and $\beta$ be the bond-stretching and bond-bending constants as defined by Martin.[19] The elastic energy for the strain of Eq. (4) is, for these materials,

$$F=(6\epsilon^2/a)\,[\alpha(1-\zeta)^2+\beta(1+\zeta)^2] . \tag{B1}$$

By minimizing Eq. (B1) with respect to $\zeta$, one obtains the internal strain parameter $\zeta_0$ for pure Si and Ge:

$$\zeta_0=(\alpha-\beta)/(\alpha+\beta) . \tag{B2}$$

For a doped material we must add to Eq. (B1) the free-carrier contribution which we shall represent, in general, by

$$\Delta F=-(6\mathfrak{a}/a)\,\mathfrak{D}^2 , \tag{B3}$$

where the constant $\mathfrak{a}$, which depends on doping, has been treated in Sec. II for the various cases of interest, and $\mathfrak{D}$ is the deformation potential defined by Eq. (5). The dependence of $\zeta$ on doping arises through the dependence of $\mathfrak{D}$ on $\zeta$ given in Eq. (5). By minimizing the sums of Eqs. (B1) and (B3) with respect to $\zeta$, we obtain

$$\zeta=\frac{\alpha-\beta-\mathfrak{a}\mathfrak{D}'(\mathfrak{D}_0/4)}{\alpha+\beta-\mathfrak{a}(\mathfrak{D}_0/4)^2} . \tag{B4}$$

Since $\mathfrak{a}$ is the parameter responsible for the small changes in $C_{44}$ obtained in Sec. II, we can expand Eq. (B4) in power series of $\mathfrak{a}$ to first order (an expansion of $\zeta$ up to first order in $\mathfrak{a}$ gives free energies and elastic constants correct to second order in $\mathfrak{a}$):

$$\zeta=\zeta_0(1-\lambda) , \tag{B5}$$

where

$$\lambda = [\alpha\bar{\mathfrak{D}}/(\alpha-\beta)]\,(\mathfrak{D}_0/4), \quad \bar{\mathfrak{D}} = \mathfrak{D}' - \tfrac{1}{4}\zeta_0\mathfrak{D}_0 \,. \qquad \text{(B6)}$$

Substituting Eq. (B5) into the expression for the free energy of the doped crystal and retaining terms up to second order in $\alpha$ alone, we obtain the modified free energy which, in turn, is compared with Eq. (10) to yield the change in the elastic constant $C_{44}$:

$$\frac{\Delta C_{44}}{C_{44}} = \frac{\delta^{(1)}C_{44}}{C_{44}} - \frac{4\alpha\beta}{(\alpha+\beta)^2}\left(\frac{\mathfrak{D}_0/4}{\bar{\mathfrak{D}}}\right)^2\left(\frac{\delta^{(1)}C_{44}}{C_{44}}\right)^2 , \qquad \text{(B7)}$$

where $\delta^{(1)}C_{44}$ is the first-order change in $C_{44}$ computed in Sec. II and given by

$$\delta^{(1)}C_{44} = -(1/a)\alpha\bar{\mathfrak{D}}^2 \,. \qquad \text{(B8)}$$

The second term on the right-hand side of Eq. (B7) gives the contribution to $C_{44}$ of changes in $\zeta$ with doping. Using for $\alpha$ and $\beta$ the values obtained by Martin[19] and for $\delta^{(1)}C_{44}$ the expressions derived in Sec. II, we find that this term is always less than $2\times10^{-4}$; i.e., even in the best of cases (greatest attainable dopings), the contributions of the change of $\zeta$ with doping to $C_{44}$ is less than one hundredth of the first-order contributions computed in Sec. II. Such small contributions are undetectable. On the other hand, Eq. (B5) predicts changes in the parameter $\zeta$ with doping given by

$$\Delta\zeta = \frac{4\alpha\beta}{(\alpha+\beta)^2}\left(\frac{\delta^{(1)}C_{44}}{C_{44}}\right)\left(\frac{\mathfrak{D}_0/4}{\bar{\mathfrak{D}}}\right) , \qquad \text{(B9)}$$

which can mean a decrease in $\zeta$ of 6% for the most heavily doped $p$-type materials. The parameter $\zeta$ has been measured experimentally by Segmüller[30] in pure Si and Ge. The change in $\zeta$ predicted by Eq. (B9) could be detected by performing analogous measurements on heavily doped materials.

†Work supported by the NSF and the Army Research Office, Durham, N. C.

*Present address: Max Planck Institut für Festkörperforschung, Stuttgart, Germany.

[1]R. W. Keyes, in *Solid State Physics*, Vol. 20, edited by F. Seitz and D. Turnbull (Academic, New York, 1967), p. 37.

[2]G. E. Pikus, Zh. Eksperim. i Teor. Fiz. 41, 1258 (1961) [Sov. Phys. JETP 14, 898 (1962)].

[3]L. J. Bruner and R. W. Keyes, Phys. Rev. Letters 101, 944 (1956).

[4]N. G. Einspruch and C. Czavinsky, Appl. Phys. Letters 2, 1 (1963); Phys. Rev. 132, 2434 (1963).

[5]J. R. Drabble and J. Fendley, Solid State Commun. 3, 269 (1965).

[6]J. J. Hall, Phys. Rev. 137, A960 (1965).

[7]V. M. Beilin, Yu Kh Velikov, and O. M. Krasil'nikov, Fiz. Tverd. Tela 12, 684 (1970) [Sov. Phys. Solid State 12, 531 (1970)].

[8]G. Weinreich, T. M. Sanders, Jr., and H. G. White, Phys. Rev. 114, 33 (1959).

[9]D. Long, *Energy Bands in Semiconductors* (Interscience, New York, 1968), Chap. 5.

[10]M. Cardona and F. H. Pollak, Phys. Rev. 142, 530 (1966).

[11]N. S. Nagendra Nath, Proc. Indian Acad. Sci. 1, 333 (1934).

[12]R. A. Cowley, J. Phys. (Paris) 26, 659 (1965).

[13]T. R. Hart, R. L. Aggarwal, and B. Lax, Phys. Rev. 1, 638 (1970).

[14]J. C. Hensel, H. Hasegawa, and M. Nakayama, Phys. Rev. 138, A225 (1965).

[15]L. Laude, F. H. Pollak, and M. Cardona, Phys. Rev. B 3, 2623 (1971).

[16]I. Goroff and L. Kleinman, Phys. Rev. 132, 2283 (1963).

[17]P. J. Melz, J. Phys. Chem. Solids 32, 209 (1971).

[18]F. Cerdeira and M. Cardona (unpublished).

[19]R. Martin, Phys. Rev. B 1, 4005 (1970); the constant $C_{44}^{*}$ defined in this reference differs from Eq. (8) by the factor $(1-\zeta^2)$.

[20]G. L. Bir and A. Tursunov, Fiz. Tverd. Tela 4, 2625 (1962) [Sov. Phys. Solid State 4, 1925 (1963)].

[21]J. McDougall and E. Stoner, Phil. Trans. Roy. Soc. (London) A237, 67 (1938).

[22]H. Brooks, in *Advances in Electronics and Electron Physics*, edited by L. Marton (Academic, New York, 1955), Vol. 7, p. 85.

[23]C. W. Higginbotham, Ph. D. thesis (Brown University, 1970) (unpublished).

[24]F. H. Pollak and M. Cardona, Phys. Rev. 172, 816 (1968).

[25]J. A. Van Vechten, Phys. Rev. 182, 891 (1969).

[26]C. J. Buchenauer, F. Cerdeira, and M. Cardona, in International Conference of Light Scattering in Solids, Paris, 1971 (unpublished).

[27]R. K. Ray, R. L. Aggarwal, and B. Lax, Bull. Am. Phys. Soc. 16, 334 (1971).

[28]E. Anastassakis, A. Pinczuck, E. Burstein, F. H. Pollak, and M. Cardona, Solid State Commun. 8, 133 (1970).

[29]F. Cerdeira, C. J. Buchenauer, F. H. Pollak, and M. Cardona, Phys. Rev. B 5, 580 (1972).

[30]A. Segmüller, Phys. Kondensierten Materie 4, 63 (1965); A. Segmüller and H. R. Neyer, *ibid.* 3, 379 (1965)

[31]D. Brust, Phys. Rev. 134, A1337 (1964).

[32]A. O. E. Animalu and V. Heine, Phil. Mag. 12, 1249 (1965).

[33]V. Heine and R. O. Jones, J. Phys. C 2, 719 (1969).